CHAPTER VII

ANTIPROLIFERATIVE AND PRO-APOPTOTIC STUDIES OF COX AND 5-LOX DUAL INHIBITORY DAMMARANE TRITERPENOID 1 ON MIA PACA-2 PANCREATIC AND DU145 PROSTATE CANCER CELL LINES

7.1. AIM AND OBJECTIVES

- To evaluate antiproliferative effect of COX and 5-LOX dual inhibitory dammarane triterpenoid 1 on various cancer cell lines and non-cancerous cell line
- To evaluate pro-apoptotic effect of COX and 5-LOX dual inhibitory dammarane triterpenoid 1 in MIA PaCa-2 pancreatic and DU145 prostate cancer cells
- To evaluate the effect of COX and 5-LOX dual inhibitory dammarane triterpenoid 1 on LTB4 and PGE2 production in cancer cells

7.2. INTRODUCTION

Cancer has been considering as world health burden by World Health Organization (WHO) and it represents one of the leading causes of mortality and morbidity worldwide, with approximately 14 million new cases and 8.2 million cancer related deaths annually(Bernard and Christopher, 2014; WHO, 2015). The number of new cases is expected to rise by about 70% over the next two decades. Global action plan (2013-2020) is formed by WHO and the International Agency for Research on Cancer (IARC) in collaboration with other United Nations (UN) organization, such as UN Noncommunicable Diseases Interagency taskforce (2014), to prevent and control of noncommunicable diseases (NCDs) including, cancer in the world. These efforts are aimed to coordinate and conduct research on the causes of human cancer and the mechanisms of carcinogenesis and develop scientific strategies for cancer prevention and control, generate new knowledge, and disseminate existing knowledge to facilitate the delivery of evidence-based approaches to cancer control (WHO, 2013, 2015). In this scenario, several research groups all over the world have been working to

understand the mechanism involved in carcinogenesis and cancer progression, and developing many strategies for prevention and therapy of cancer (Block et al, 2015).

Cancer initiation and progression are multistep processes and are regulated by different internal factors, including growth factors and their receptors, cytokines, chemokines, transcriptional factors, nuclear receptors, as well as arachidonic acid (AA) derived lipid mediators (Wang and Dubois, 2010, Claus and Ambra, 2011, Weber et al., 2010, Cuendet and Pezzuto, 2000, Fabio et al., 2006). Moreover, several external factors, such as cigarette, food carcinogens, environmental factors and certain chemicals, induce various types of cancers by activating several pro-tumorigenic factors including AA pathway (Fabio et al., 2006). Molecular studies demonstrated the key role of arachidonate cascade in several cancers (Williams et al., 1999; Xian et al., 2003; Korotkova et al., 2014). Arachidonic acid metabolites (PGs and LTs) have implicated in various pathophysiological processes related to carcinogenesis and antiapoptotic activities. COX-2 and 5-LOX enzymes are up-regulated in cancer and their genes knockouts cannot disrupt normal cellular and physiological functions in mice with deficient of inflammatory response thus arachidonic acid metabolizing enzymes (PLA2, COX and 5-LOX) are the best target for development of drugs for some of the cancers (Karin et al., 2014; Barker et al., 2012). PLA_2 inhibition would theoretically prevent release of arachidonic acid (Meyer, 2005). However, several clinical studies demonstrated that some PLA_2 inhibitors are ineffective in suppression of arachidonic acid metabolites (Titsworth et al, 2008). COX-2 selective inhibition is more advantageous because COX-1 is a constitutive enzyme. However, recent reports demonstrated that both COX-1 and COX-2 enzymes play vital roles in carcinogenesis. Recent studies demonstrated that COX inhibition caused increase in leukotrines production from arachidonic through the 5-LOX pathway as a result of metabolic pathway diversion (Cianchi et al., 2006; Kit et al., 2012). In the same way, 5-LOX inhibitor like zileuton, increases the availability of arachidonic acid to cyclooxygenase enzyme that leads to increase the production of PGs. Only COX or 5-LOX inhibitors are ineffective and cause adverse effects. Thus development of safer and effective drugs that inhibit both COX-2 and 5-LOX would be advantageous due to blocking of both PGs and LTs metabolic pathways (Cianchi et al., 2006; Kit et al., 2012).

Previous studies suggest that COX and 5-LOX promotes proliferation of cancer cells and inhibit apoptosis of cancer cells (**Figure 7.1** and **7.2**). COX and 5-LOX inhibitors have been reported for anticancer and proapoptotic activities in several cancers apart from anti-inflammatory activity (Xian et al., 2003; Korotkova et al., 2014). Flavocoxid, a dual inhibitor of COX and 5-LOX suppresses TNF- α mRNA levels in macrophages. Moreover, *in vivo* studies proved the anticancer activity of flavocoxid on prostate cancer (Altavilla et al., 2012). *In vitro* and *in vivo* studies proved that a 5-LOX and COX-2 dual enzyme inhibitor, 7-*tert*-butyl-2, 3-dihydro-3, 3-dimethyl substituted dihydrofuran 30 (DHDMBF30) showed antiproliferative activity in pancreatic cancers (Zhang et al., 2008). Licofelone, a dual COX and 5-LOX inhibitor (currently under clinical trials), induces apoptosis in HCA-7 colon cancer cells (15). COX and 5-LOX inhibitory chebulagic acid from *Terminalia chebula* Retz. induces apoptosis in COLO-205 colon cancer cells (Reddy et al., 2009).

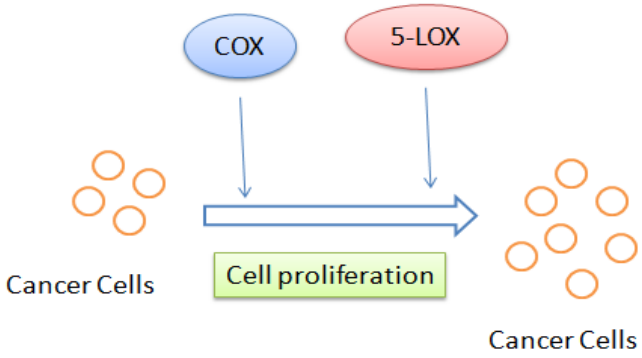

Figure 7.1. COX and 5-LOX promote proliferation of cancer cell

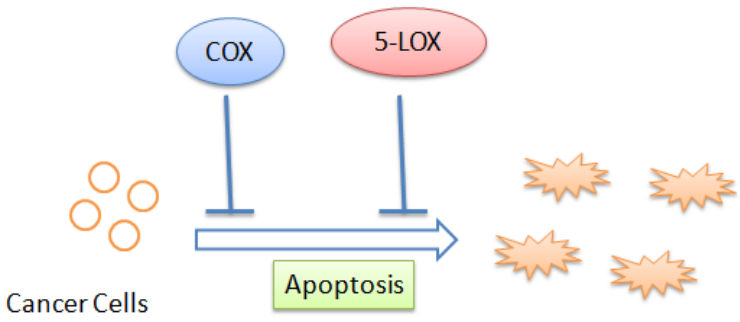

Figure 7.2. COX and 5-LOX inhibit apoptosis of cancer cells

In the present study, antiproliferative effect of isolated dammarane triterpenoid 1 on various cancer cell lines, including MIA PaCa-2 pancreatic, human promyelocytic leukemia HL-60, Caco-2 colon and DU145 prostate cancer cell lines, was evaluated. Further pro-apoptotic studies of dammarane triterpenoid 1 were performed in MIA PaCa-2 pancreatic and DU145 prostate cancer cells.

7.3. MATERIALS AND METHODS

7.3.1. Chemicals and reagents

RPMI 1640, fetal bovine serum (FBS), phosphate buffered saline (PBS), antibiotics (pencillin and streptomycin) were procured from Gibco BRL (CA, USA). MTT (3-(4,5-dimethylthiazol-2-yl)-2,5-diphenyl tetrazolium bromide), bovine serum albumin (BSA), β-actin antibodies, agarose, ethidium bromide and trypsin were procured from Sigma-Aldrich Chemical Company, (St. Louis, MO, USA). Cytochrome *c*, Bcl-2 and Bax antibodies were purchased from Santa Cruz Biotechnology (Santa Cruz, CA, USA). Nitrocellulose membrane was purchased from Millipore (Banglore, Karnataka, India). All solvents and chemicals used in experiments were of analytical grade and purchased from local suppliers.

7.3.2. Preparation of compound for anticancer studies

The compound was dissolved in dimethyl sulfoxide (DMSO) and tested up to 50 µM for MTT assay. Pro-apoptotic studies of dammarane triterpenoid 1 on DU145 prostate cancer cells were conducted at 5 and 10 µM concentration. Pro-apoptotic studies of dammarane triterpenoid 1 were conducted at single dose in MIA PaCa-2 pancreatic cancer cells due to low availability of compound. Camptothecin was used as the positive control.

7.3.3. Cancer cell lines

MIA PaCa-2 pancreatic, MCF-7 breast and DU145 prostate human cancer cell lines, and RWPE-1 human normal prostate epithelial cell line, were obtained from American Type Culture Collection (ATCC, Manassas, VA, USA).

Human promyelocytic leukemia HL-60 and Caco-2 colon were procured from European Collection of Cell Cultures (ECACC, Salisbury, Wiltshire, UK). These cancer cells were maintained in RPMI medium supplemented with 10% FCS, 100 units pencillin and 100 µg of streptomycin per ml of medium. The cells were maintained in 95% humidity with CO_2 at 37 ^{0}C temperature.

7.3.4. Cell proliferation by MTT assay

MTT assay was performed to assess the antiproliferative activity of isolated compound (Mosmann, 1983). Cancer cells were treated with isolated compound at various concentrations for 48 h. 20 µl of freshly prepared MTT reagent was added to cells and incubated at 37 °C for 2 h. The supernatant growth medium was removed and replaced with DMSO (100 µl) to dissolve the formazan crystals. The optical density (absorbance) was read at 570 nm (Mosmann, 1983).

7.3.5. Cell cycle analysis

Cancer cells ($1x10^6$/ml) were treated with the isolated compound for 24 h at concentrations of 5 µM. Compound treated cells were fixed in 70% alcohol (ice-cold) in phosphate buffered saline. Further, cells were digested with DNase free RNase (400 µg/ml) at 37 ^{o}C for 45 min and propidium iodide (10 µg/ml) was added to the cells in dark. Propidium iodide-DNA fluorescence in cancer cells was analyzed by flow cytometerically using BD FACS CALIBUR (Becton Dickinson, Franklin Lakes, New Jersey, USA). The apoptotic cell population was determined by fluorescence intensity of sub-G0 phase cells using flow cytometer (Bhushan et al.,2006).

7.3.6. Mitochondrial membrane potential changes ($\Delta\Psi m$) measurement assay

Mitochondrial membrane potential changes ($\Delta\Psi m$) were determined by flow cytometer using rhodamine-123 (green-fluorescent dye) (50). Cancer cells ($1x10^6$ cells/well) were exposed to isolated compound (5 µM) for 24 h. Further, Rhodamine-123 (200 nM) was added to the cells and kept in dark for 35 min. The cells were further centrifuged and the obtained pellet was washed with phosphate buffered saline (1 ml). The intensity of fluorescence in the cells represents the mitochondria membrane potential change ($\Delta\Psi m$), was measured using flow cytometer (Tong et al., 2004).

7.3.7. Hoechst 33258 staining of cells for nuclear morphology

Cancer cells (1×10^6 cells/ml/12 well plate) were treated with isolated compound for 24 h. The treated cells were centrifuged at 300 g for 5 min and washed with phosphate buffered saline. Further, collected MIA PaCa-2 pancreatic cancer cells were gently suspended in phosphate buffered saline (100 µl) and fixed in a solution contained acetic acid (cold): methanol (1+3, v/v) (400 µl) and kept overnight at 4 °C. Cells were spread on a clean slide and dried for 10 h at room temperature. Hoechst stain solution (1 ml) was placed on cells, which were spread on slide and kept for 30 min at room temperature under subdued light. The slides were washed properly to remove unwanted stain and mounting fluid (50 µl) (PBS in glycerol (1:1)) was added on cells, followed by covered with cover slip, which was further sealed with nail polish (before observing under microscope). The prepared slides were kept under inverted fluorescence microscope (Olympus 1X70) to observe the nuclear morphological alterations and apoptotic bodies in cancer cells (Tong et al., 2004).

7.3.8. Western blot analysis for Cytochrome *c*/Bcl-2/Bax expression studies

Cancer cells were treated with isolated compound for 24 h. Further, washed with PBS and suspended in a lysis buffer containing 20 mM Tris, 1mM EDTA, 150 mM NaCl, 0.5% deoxycholic acid, 1% Triton X-100, 1mM glycerophosphate, 1mM sodium orthovanadate, 1mM phenylmethylsulfonyl fluoride (PMSF), 10 mg/ml leupeptin and 20 mg/ml aprotinin for 30 min at 4 ^{0}C. Then the buffer mixture was centrifuged at 10,000 g for 10 min. The collected supernatant contained cell lysate, which was used in estimation of cytochrome *c*. Equal amount of protein from cell lysate was subjected to SDS-PAGE (8-12%) and the electrophored gel was transferred on to nitrocellulose membranes. The blotted membranes were blocked with non-fat milk (5%) to prevent nonspecific binding followed by incubated with cytochrome *c*/Bcl-2/Bax primary antibodies in antibody diluted buffer (the buffer composed of Tris-buffered saline (TBS), 0.05% Tween-20 and 5% fat free dry milk) at 4 ^{0} C for 8-12 h. After that, the blots were incubated with appropriate conjugated secondary antibodies (horseradish peroxidase-conjugated). Western blotting detection reagents were used to detect the signals (Reddy et al., 2009).

7.3.9. **Cytosolic cytochrome *c* estimation using ELISA technique.**

Cells were collected by centrifugation at 600 *g* for 5 min at 4 ºC. The cell pellets were washed once with ice-cold PBS and resuspended in cytosol extraction buffer (20 mM Hepes-KOH, pH 7.5, 10 mM KCl, 1.5 mM $MgCl_2$, 1 mM sodium EDTA, 1 mM sodium EGTA, 1 mM dithiothreitol and 0.1 mM PMSF) containing 250 mM sucrose on ice for 10 min. The cells were homogenized with the grinder on ice. Further, the homogenates were centrifuged at 700 *g* for 10 min at 4 ºC. The supernatants were centrifuged at 10,000 x g for 30 min at 4 ˚C. Supernatant was collected as cytosolic fraction.

Cytosolic cytochrome *c* levels were determined using quantitative sandwich enzyme immunoassay using microplate reader. Sample or standard (100 µL) was added into each well and incubated for 2 h at room temperature. The wells were washed several times with wash buffer. The plate was inverted and cleaned with paper toweling. Cytochrome *c* conjugate (200 µL) was added into each well and incubated for 2 h at room temperature. Wells were washed several times with wash buffer. Substrate solution (200 µL) was added into each well and incubated for 30 min at room temperature. Finally, stop solution (50 µL) was added into wells. The optical density (absorbance) of each well was determined using microplate reader at a 450 nm wavelength (Aysegul et al., 2012).

7.3.10. **Caspases assays**

Caspases-3, -8 and -9 assays were measured according to manufacturer`s instructions using a caspase colorimetric protease kit (Abcam, Cambridge, MA, USA). Cells were treated with compounds for 48 h. The cells were lysed by the addition of 50 µL of chilled cell lysis buffer and incubated on ice for 10 min. The resulting cell lysate was centrifuged for 1 min at 10,000 *g*, and the supernatant was collected. The cell lysate containing 75 mg of protein was incubated with 4 mL of 4 mmol/L pNA-conjugated substrates (DEVD-pNA, IETD-pNA and LEHD-pNA; substrates for caspase-3, -8 and -9, respectively) at 37°C for 3 h. The amount of pNA released was measured at 405 nm using an ELISA microplate reader (Bio rad). The caspases activity was expressed as fold difference (Aysegul et al., 2012; Heydar et al., 2013).

7.3.11. **Quantification of Bcl-2.**

The intracellular content of Bcl-2 was quantified using the human Bcl-2 ELISA kit (Abcam, Cambridge, MA, USA). For the sample preparation, the cells were lysed with 1X lysis buffer. After 1 h of incubation at room temperature, the sample was spun at 1,000 g for 15 min and the supernatant was used for Bcl-2 measurement. Briefly, 80 µL of sample diluent and 20 µL of sample were added into the wells coated with monoclonal antibody to human Bcl-2, and after that the wells were washed twice with the wash buffer. Next, 50 µL of biotin-conjugate were added into the wells. After 2 h of incubation at room temperature on a microplate shaker, 100 µL of streptavidin-horseradish peroxidase were added. The sample was incubated again for 1 h at room temperature on a microplate shaker. The solution was withdrawn and the wells were washed with 3X wash buffer. Immediately, 100 µL of TMB substrate solution were added. Finally, 100 µL of stop solution were added into each well to stop the enzyme reaction. The absorbance was read using an ELISA reader at 450 nm wavelengths. Bcl-2 protein concentration was determined from the standard protein graphic using the optical densities of the samples (Aysegul et al., 2012).

7.3.12. Quantification of Bax.

Bax protein concentration determination was carried out using the Human Bax Enzyme Immunometric Assay kit (Assay Designs, Ann Arbor, MI, USA). The lysate (sample) preparation was carried out according to the manual. Following centrifugation (16,000 g for 15 min), the cells were resuspended in Modified Cell lysis buffer 4 (0.5 µL/mL of Sigma Protease Inhibitor Cocktail and 1 mM phenyl-methylsulfonyl fluoride (PMSF)). Cell lysate (100 µL) (sample) was added into the wells coated with monoclonal antibody to human Bax-α in triplicate. The plate was tapped gently to mix the contents. The sample was incubated at room temperature on a plate shaker for 1 h. The wells were emptied and washed with 5X wash buffer. After the final wash, the plate was tapped gently on a lint free paper towel to remove any remaining wash buffer. The sample was incubated again for 1 h at room temperature on a plate shaker after the addition of 100 µL of specific antibody (biotinylated monoclonal antibody to Bax-α) into each well. The wells were washed again with 5X wash buffer and emptied. Next, 100 µL of blue conjugate (streptavidin conjugated to horseradish peroxidase) was added into each well. The sample was left on a plate shaker for 30 min at room temperature. The wells were washed again as in the

previous step. Solution (100 µL) of 3,3',5,5' tetramethylbenzidine (TMB) and H_2O_2 was added into each well. Finally, 100 µL of stop solution containing hydrochloric acid in water was added to stop the enzyme reaction. The optical densities were read at 450 nm using an ELISA reader. Bax protein concentration was determined from the standard protein graphic using the optical densities of the samples (Aysegul et al., 2012).

7.3.13. DNA agarose gel electrophoresis

Apoptosis in cancer cells was assessed by DNA fragmentation using agarose gel electrophoresis (Reddy et al., 2009). Cancer cells were treated with isolated compound for 24 h. Treated cancer cells were centrifuged at 400 *g* for 5 min, washed with PBS contained 20 mM EDTA. The collected pellet was dissolved in 250 µl of lysis buffer containing 100mM NaCl, 5mM EDTA, 10mM Tris–HCl (pH 8.0), and 5% Triton X-100 and then incubated with 100 µg/ml DNase-free RNase at 37 ^{0}C for 90 min. Further, buffer mixture containing cell lysate was treated with proteinase-K (200 µg/ml) for 1 h at 50 ^{0}C. Phenol: chloroform: isoamyl alcohol (1:24:1) solution mixture used to extract the DNA from cells and centrifuged at 13000 *g* for 2 min. DNA was extracted as precipitate from aqueous phase with addition of 3 volumes of ice-cold alcohol and sodium acetate (0.3M) at -20 °C for 12 h. The precipitate containing DNA was centrifuged at 13,000 *g* for 10 min. Further, the pellet containing DNA was dissolved in Tris-EDTA buffer (50 µl) and run on the agarose gel (1.8%) electrophoresis for 1 h at 70 V. Ethidium bromide (EtBr) was used for staining of DNA and bands were observed under transilluminator (Reddy et al., 2009).

7.3.14. Quantification of Leukotriene B4

Leukotriene B4 levels were quantified in cell culture supernatant using leukotriene B4 competitive ELISA kit (Cayman chemical, USA). The detailed protocol was mentioned in **Chapter 6.7.4.** (Maclouf, 1987).

7.3.15. Quantification of Prostaglandin E_2

Prostaglandin E2 (PGE2) levels were quantified in cell culture supernatant using Prostaglandin E2 competitive ELISA kit (Cayman chemical, USA). The detailed protocol was mentioned in **Chapter 6.7.5.** (Hamberg, 1971).

7.3.16. Statistical analysis

Experimental results were expressed as mean (n = 3-6) ± standard error mean (S.E.M). The difference between experimental groups was compared by one-way analysis of variance (ANOVA). The *p* value ≤0.05 was considered as significant.

7.4. RESULTS

7.4.1. Antiproliferative activity of dammarane triterpenoid 1 on various cancer cell lines

Antiproliferative activity of dammarane triterpenoid 1 was assessed by MTT assay and found significant anti-proliferative profile on various cancer cell lines. As shown in **Figure 7.3**, dammarane triterpenoid 1 exhibited good anti-proliferative activity with IC_{50} of 12.36±0.33, 14.3±0.22, 19.9±0.62, 20.43±3.21 and 25.6±1.68 µM for MIA PaCa-2 pancreatic, DU 145 prostate, Caco-2 colon, MCF-7 breast and HL-60 leukemia cancer cell lines respectively. Dammarane triterpenoid 1 exhibit less antiproliferative effect on RWPE-1 human normal prostate epithelial cell line (IC_{50} = 83.37±8.21 µM) as compared its effect on DU 145 prostate cancer cell line. This demonstrated that dammarane triterpenoid 1 exhibits significant antiproliferative on cancerous cells than normal cells. Campothecin was used as positive control. Dammarane triterpenoid 1exhibits comparable antiproliferative effect on cancerous cells with camptothecin and very less potential where in case of non-cancerous cell line. Dammarane triterpenoid 1 showed significant antiproliferative activity on MIA PaCa-2 pancreatic and DU145 prostate cancer cell line among tested cancer cell lines (**Figure 7.3**). Thus, further some of the pro-apoptotic studies were carried out on MIA PaCa-2 pancreatic and DU145 prostate cancer cells (**Figure 7.3**).

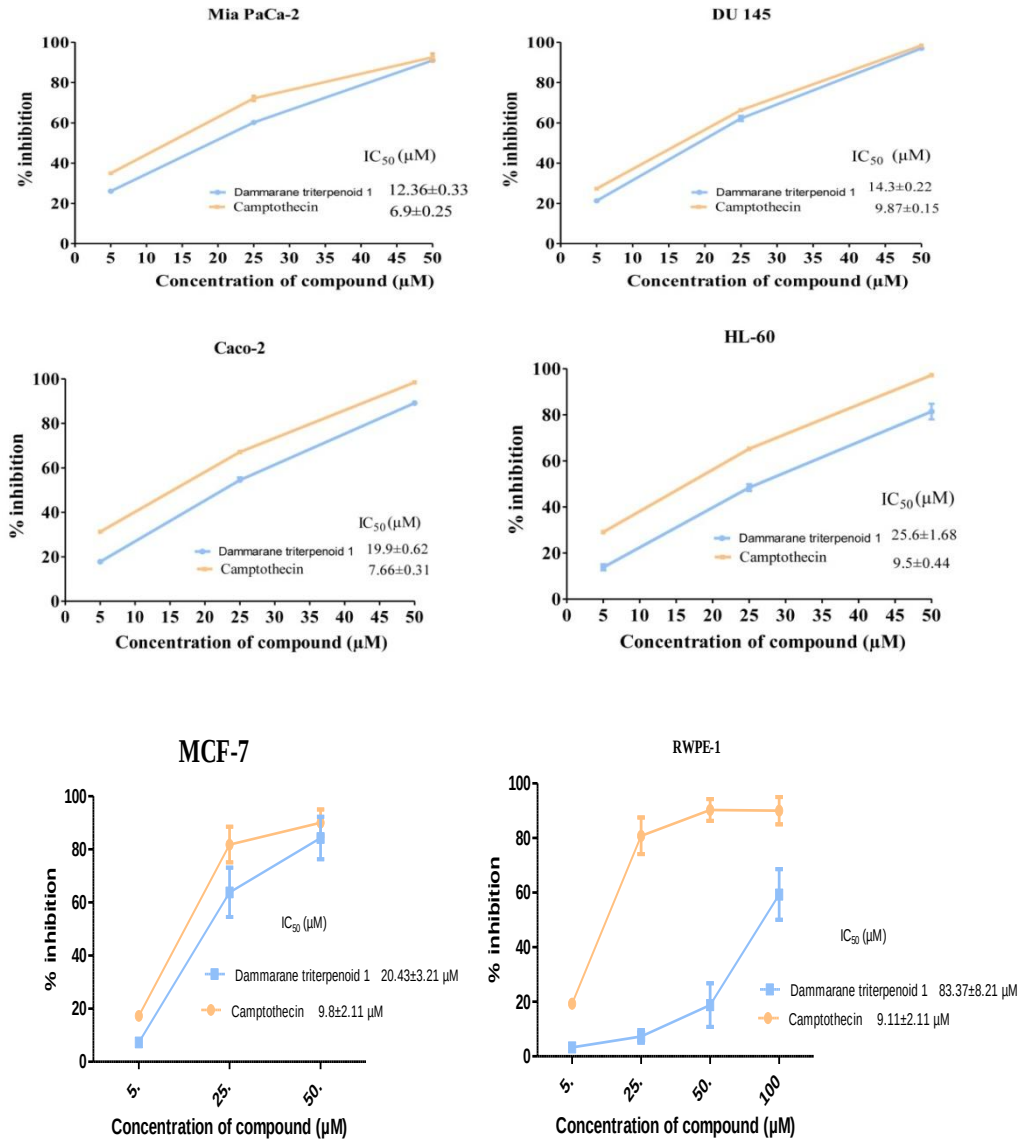

Figure 7.3. Antiproliferative effect of dammarane triterpenoid 1 on MIA PaCa-2 pancreatic, DU 145 prostate, Caco-2 colon HL-60 leukemia and MCF-7 breast cancer cell lines, as well as RWPE-1 human non-cancerous prostate epithelial cell line in dose-dependent manner.

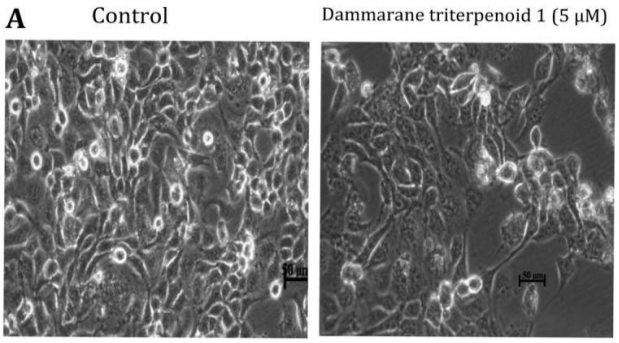

Figure 7.4. Growth of untreated (control) and dammarane triterpenoid 1 treated (5 µM) pancreatic cancer cells were observed under inverted microscope (X20).

7.4.2. Apoptosis inducing activity of dammarane triterpenoid 1 in MIA PaCa-2 pancreatic cells

7.4.2.1. Effect of dammarane triterpenoid 1 on cell cycle of MIA PaCa-2 pancreatic cancer cells

Flow cytometric graphs representing cell cycle distribution of different phase populations (G0/G1, S, G2/M) in untreated (control) and treated (5 µM) pancreatic cancer cells. Sub-G_0 cell phase population represents the apoptotic population is high in treated pancreatic cancer cells (15%) at 5 µM of dammarane triterpenoid 1 compared to untreated (control) (**Figure 7.5**). Camptothecin (positive control) caused 69% accumulation of sub-G_0 phase cell population (data not showed). The sub-G_0 population accumulation is an indicator of apoptotic inducing activity of dammarane triterpenoid 1 in MIA PaCa-2 pancreatic cancer cells.

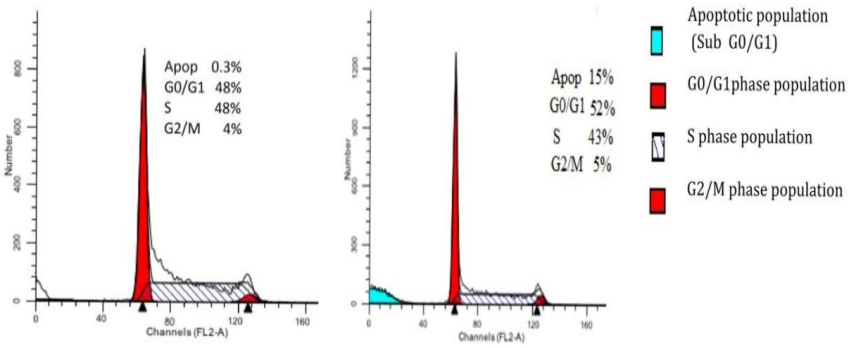

Figure 7.5. Effect of dammarane triterpenoid 1 on cell cycle of MIA PaCa-2 pancreatic cancer cells

7.4.2.2. Effect of dammarane triterpenoid 1 on mitochondrian membrane potential (ΔΨm) in MIA PaCa-2 pancreatic cancer cells

In flow cytometric analysis (**Figure 7.6**), dammarane triterpenoid 1 (5 µM) caused 29% of mitochondria membrane potential loss in MIA PaCa-2 pancreatic cells compared to untreated cells (control). Camptothecin (positive control) caused 61% mitochondrian membrane potential loss at 4 µM concentration (data was not showed). The mitochondria membrane potential loss is an indicator of apoptotic inducing activity of dammarane triterpenoid 1 in MIA PaCa-2 pancreatic cancer cells.

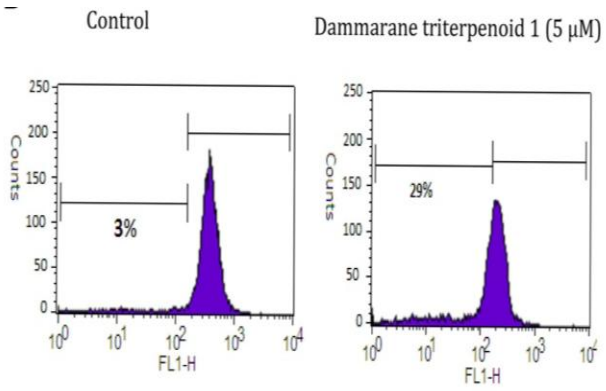

Figure 7.6. Mitochondria membrane potential loss representing flow cytometric graphs of treated cells (5 µM) of pancreatic cancer as comparing to untreated cells (control).

7.4.2.3. Effect of dammarane triterpenoid 1 on nuclear morphology of MIA PaCa-2 pancreatic cancer cells

In nuclear morphological studies, Hoechst stain that selectively binds DNA and visualizes the nuclear morphological changes under fluorescence microscopy. Dammarane triterpenoid 1 (5 µM) caused nuclear condensation and blebbing indicating the formation of apoptotic bodies in MIA PaCa-2 pancreatic cancer cells as shown by white arrows in **Figure 7.7**, while the nuclei of untreated cells were round in shape.

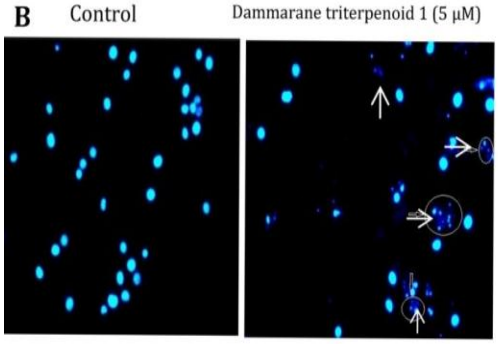

Figure 7.7. Nuclear morphological changes in untreated (control) and treated cells (5 µM) of pancreatic cancer were observed under fluorescent microscope.

7.4.2.4. Effect of dammarane triterpenoid 1 on cytosolic cytochrome *c* levels in MIA PaCa-2 pancreatic cancer cells

In western blot analysis, cytochrome *c* levels were high in dammarane triterpenoid 1 (5 µM)-treated MIA PaCa-2 cells as compared to untreated cells (**Figure 7.8**). This is a hall mark of apoptosis.

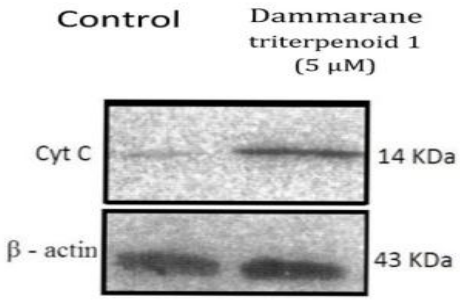

Figure 7.8. Western blot results represent the increased levels of cytosolic cytochrome *c* in treated cells as compared to control.

7.4.2.5. Effect of dammarane triterpenoid 1 on Bcl-2 levels in MIA PaCa-2 pancreatic cancer cells

Studies were undertaken to test whether Bcl-2 expression is affected after dammarane triterpenoid 1 treatment in MIA PaCa-2 pancreatic cells. Changes in the expression of anti-apoptotic Bcl-2 following dammarane triterpenoid 1 treatment were evalauted by Western blotting technique. As shown in **Figure 7.9**, dammarane triterpenoid 1 slightly reduced the expression of Bcl-2 in MIA PaCa-2 pancreatic cancer cells.

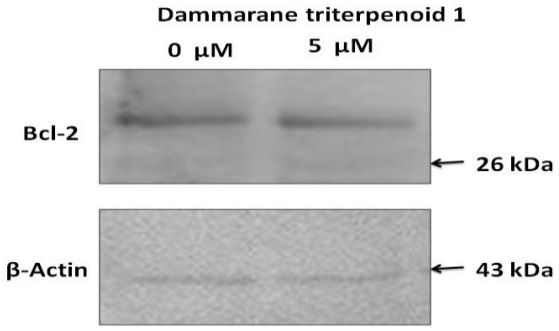

Figure 7.9. Immunoblot analysis of Bcl-2 expression in MIAPaCa-2 pancreatic cancer cells treated with dammarane triterpenoid 1

7.4.2.6. Effect of dammarane triterpenoid 1 on Bax levels in MIA PaCa-2 pancreatic cancer cells

Studies were undertaken to test whether Bax expression is affected after dammarane triterpenoid 1 treatment in MIA PaCa-2 pancreatic cells. As shown in **Figure 7.10**, dammarane triterpenoid 1 slightly enhanced the expression of Bax in MIA PaCa-2 pancreatic cancer cells. Changes in the expression of pro-apoptotic Bax following dammarane triterpenoid 1 treatment were evaluated by Western blotting technique.

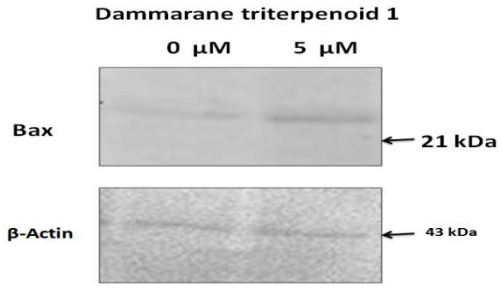

Figure 7.10. Immunoblot analysis of Bax expression in MIA PaCa-2 pancreatic cancer cells treated with dammarane triterpenoid 1

7.4.2.7. Effect of dammarane triterpenoid 1 on caspases activity in MIA PaCa-2 pancreatic cancer cells

Caspases-3 and -9 activities were high in dammarane triterpenoid 1-treated MIA PaCa-2 pancreatic cancer cells as compared to control cells (**Figure 7.11**). Dammarante triterpenoid 1 did not show any effect on caspase 8. Activation of caspases is a hall mark of apoptosis induction.

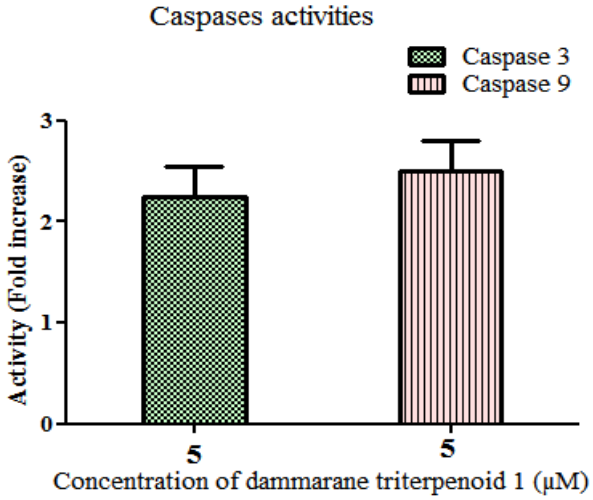

Figure 7.11. Elevation of caspases-3 and 9 activities in dammarane triterpenoid 1-treated MIA Pa-2 pancreatic cancer cells

7.4.2.8. Dammarane triterpenoid 1-induced DNA fragmentation in MIA PaCa-2 pancreatic cancer cells

Further apoptotic inducing activity of dammarane triterpenoid 1 was confirmed based on DNA agarose gel electrophoresis, DNA laddering (180-200 bp) was observed in treated MIA PaCa-2 pancreatic cancer cells where as it was absent in untreated cells (**Figure**. **7.12**).

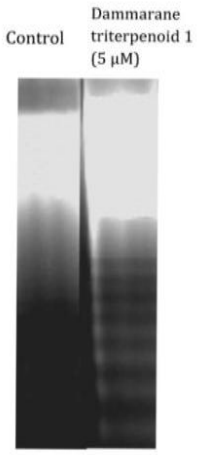

Figure 7.12. DNA fragmentation representing picture of treated cells (5 µM) compared with untreated (control) pancreatic cancer cells.

7.4.3. Effect of dammarane triterpenoid 1 on LTs levels in MIA PaCa-2 pancreatic cells

Dammarane triterpenoid 1 inhibited 50.41± 2.58% and 69.69 ± 3.20% production of LTB4 levels in MIA PaCa-2 pancreatic cancer cells at 5µM and 10µM concentrations respectively. **Figure 7.13** represents the inhibitory effect of dammarane triterpenoid 1 on LTB4 levels in MIA PaCa-2 pancreatic cancer cells.

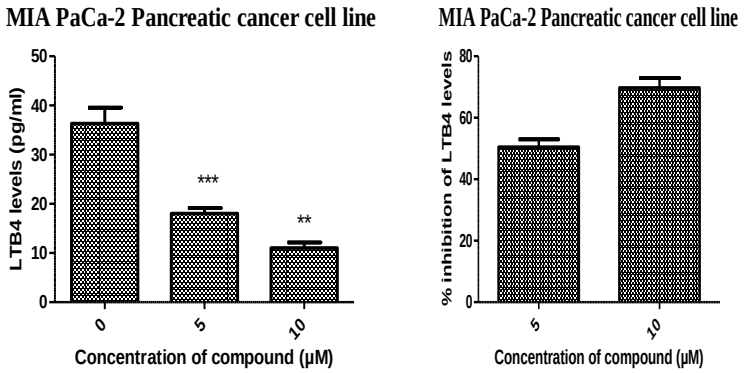

(i) (ii)

Figure 7.13. Effect of dammarane triterpenoid 1on LTB4 levels represented in pg/ml (i) and percent inhibition (ii) in MIA PaCa-2 pancreatic cancer cells

7.4.4. Effect of dammarane triterpenoid 1 on PGs levels in MIA PaCa-2 pancreatic cells

Dammarane triterpenoid 1 inhibited 24.01± 3.80% and 37.26± 4.20% production of PGE2 levels in MIA PaCa-2 pancreatic cancer cells at 5µM and 10µM concentrations respectively. **Figure 7.14** represents the inhibitory effect of dammarane triterpenoid 1 on PGE2 secretion levels in MIA PaCa-2 pancreatic cancer cells.

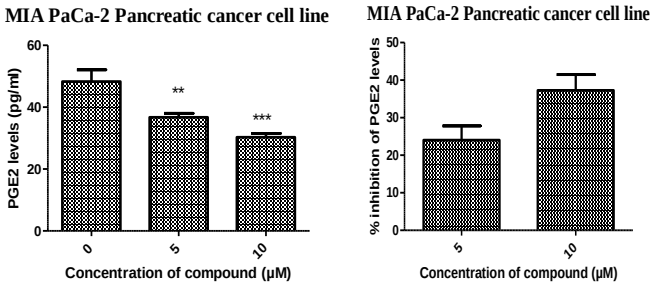

(i) (ii)

Figure 7.14. Effect of dammarane triterpenoid 1on PGE2 levels represented in pg/ml (i) and percent inhibition (ii) in MIA PaCa-2 pancreatic cancer cells

7.4.5. Pro-apoptotic potential of dammarane triterpenoid 1 in DU145 prostate cancer cells

7.4.5.1. Effect of dammarane triterpenoid 1 on cell cycle of DU145 prostate cancer cells

In cell cycle analysis using flow cytometry, dammarane triterpenoid 1 caused accumulation of DU145 prostate cancer cells in G0/G1 phase. This demonstrates that dammarane triterpenoid 1 arrested cell cycle of DU145 prostate cancer cells at G0/G1 phase (**Figure 7.15**). Sub-G_0 cell phase population represents the apoptotic population is 10% and 29% high in treated prostate cancer cells at 5 and 10 µM of dammarane triterpenoid 1 compared to untreated (control) (**Figure 7.15**). Camptothecin (positive control) caused 39% accumulation of sub-G_0 phase cell population at 5µM. The sub-G_0 population accumulation is an indicator of apoptotic inducing activity of dammarane triterpenoid 1 in DU145 prostate cancer cells.

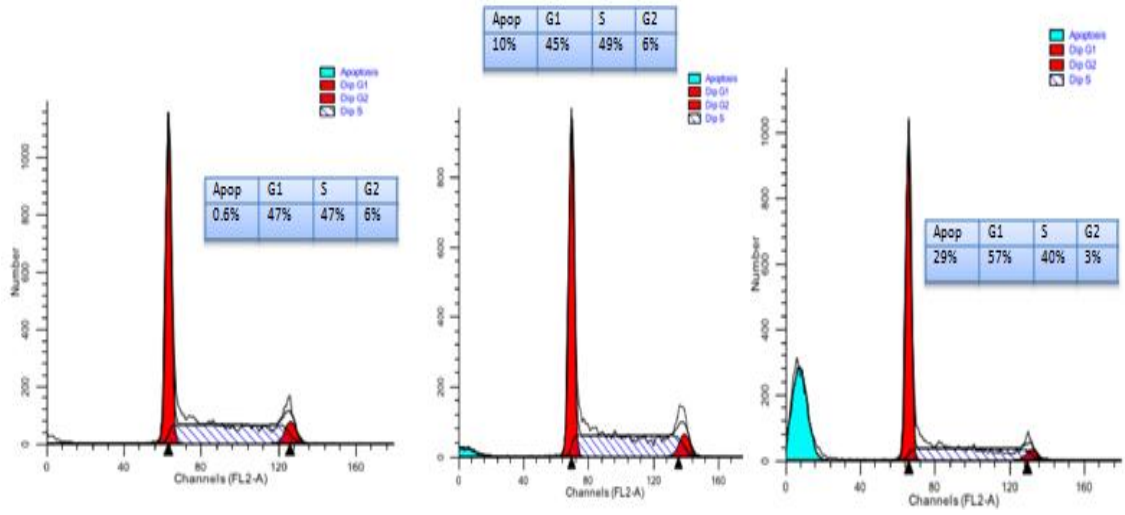

Figure 7.15. Effect of dammarane triterpenoid 1 on cell cycle of DU145 prostate cancer cells represented in flow cytometic histograms

7.4.5.2.Effect of dammarane triterpenoid 1 on mitochondrian membrane potential (*ΔΨm*) of DU145 prostate cancer cells

In flow cytometric analysis (**Figure 7.16**), dammarane triterpenoid 1 caused 28% and 55% of mitochondria membrane potential loss in DU145 prostate cancer cells compared to untreated cells (control) at 5µM and 10 µM. Camptothecin (positive control) caused 65% mitochondrian membrane potential loss at 5 µM concentration (data was not showed). The mitochondria membrane potential loss is an indicator of apoptotic inducing activity of dammarane triterpenoid 1 in DU145 prostate cancer cells.

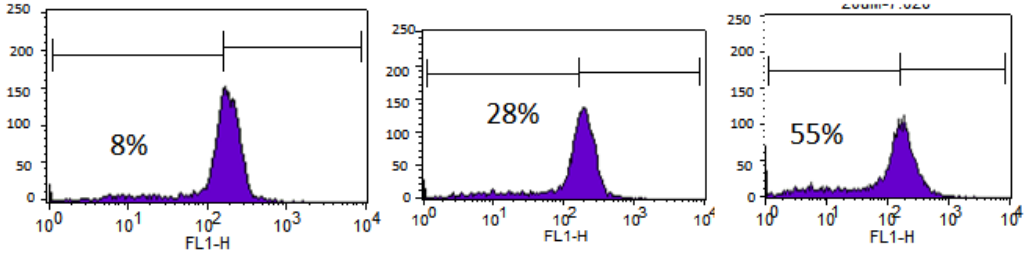

0 µM **5 µM** **10 µM**

Dammarane triterpenoid 1

Figure 7.16. Effect of dammarane triterpenoid 1 on mitochondrian membrane potential loss in DU145 prostate cancer cells represented in flow cytometric histograms

7.4.5.3. Effect of dammarane triterpenoid 1 on cytosolic cytochrome *c* levels in DU145 prostate cancer cells

Dammarane triterpenoid 1 elevates the cytosolic cytochrome *c* levels in DU145 prostate cancer cells. The data is presented in Figure 7.17, 11.46±1.1% and 30.48±2.97% increase of cytosolic cytochrome *c* levels were observed in dammarane triterpenoid 1-treated DU145 prostate cancer cells as compared to control (untreated) at 5 and 10 µM concentrations respectively(**Figure 7.17**). Camptothecin (positive control) caused 20.69± 2.59% and 38.70± 1.64% increase of cytosolic cytochrome *c* levels were observed in treated DU145 prostate cancer cells as compared to control (untreated) at 5 and 10 µM concentrations respectively

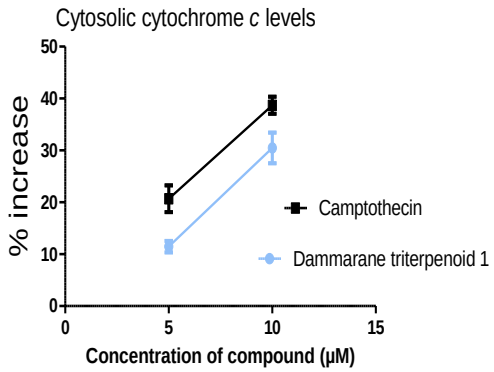

Figure 7.17. Effect of dammarane triterpenoid 1on cytochrome *c* levels represented in percent increase in treated and untreated DU145 prostate cancer cells.

7.4.5.4. Effect of dammarane triterpenoid 1 on Bcl-2 levels in DU145 prostate cancer cells

As shown in **Figure 7.18**, dammarane triterpenoid 1 decreased the Bcl-2 levels dose dependently. 16.56±1.25% and 45.16±2.79% decrease in Bcl-2 levels were observed in treated DU145 prostate cancer cells as compared to untreated cells at 5 and 10 µM concentrations respectively.

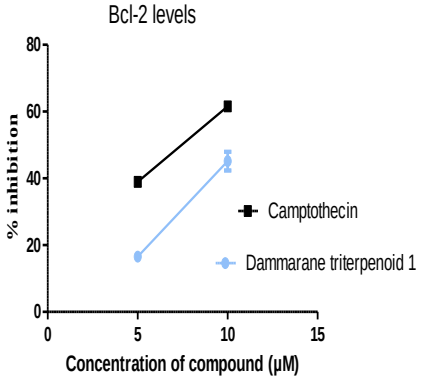

Figure 7.18. Effect of dammarane triterpenoid 1on Bcl-2 levels represented percent inhibition in treated DU145 prostate cancer cells.

7.4.5.4.1. Effect of dammarane triterpenoid 1 on Bax levels in DU145 prostate cancer cells

Dammarane triterpenoid 1 treatment caused 23.02±1.25% and 39.58±1.47% increase in Bax levels in treated DU145 prostate cancer cells as compared to untreated cells at 5 and 10 µM concentrations respectively (**Figure 7.19**). Elevation of Bax levels in dammarane triterpenoid 1-treated DU145 prostate cancer cells demonstrates apoptosis induction.

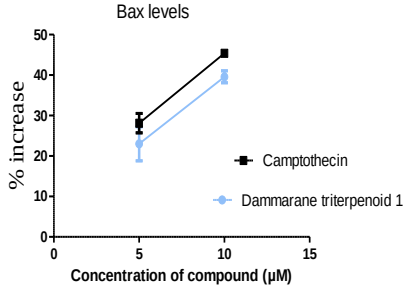

Figure 7.19. Effect of dammarane triterpenoid 1on Bax levels represented percent increase in treated DU145 prostate cancer cells.

7.4.5.5. Effect of dammarane triterpenoid 1 on caspases activity in DU145 prostate cancer cells

Caspases-3 and -9 activities were high in dammarane triterpenoid 1-treated DU145 prosate cancer cells as compared to control cells (**Figure 7.20**). Dammarante triterpenoid 1 did not show any effect on caspase 8. Activation of caspases is a hall mark of apoptosis induction.

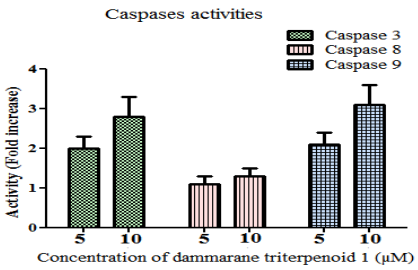

Figure 7.20. Effect of dammarane triterpenoid 1 on caspases activities in DU145 prostate cancer cells

7.4.5.6. Dammarane triterpenoid 1 induced DNA fragmentation in DU145 prostate cancer cells

DNA laddering (180-200 bp) was observed in dammarane triterpenoid 1 treated DU145 prostate cancer cells where as it was absent in untreated cells (**Figure 7.21**). The study demonstrated that dammarane triterpenoid 1 induces DNA fragmentation. This is an indication of induction of apoptosis.

Figure 7.21. Dammarane triterpenoid 1 (5 & 10 µM) caused DNA fragmentation in DU145 prostate cancer cells

7.4.6. Effect of dammarane triterpenoid 1 on LTs levels in DU145 prostate cancer cells

Dammarane triterpenoid 1 inhibited 47.47± 0.90% and 58.45± 1.20% production of LTB4 levels in DU145 prostate cancer cells at 5µM and 10µM concentrations respectively. **Figure 7.22** represents the inhibitory effect of dammarane triterpenoid 1 on LTB4 levels in DU145 prostate cancer cells. Results are statistically significant.

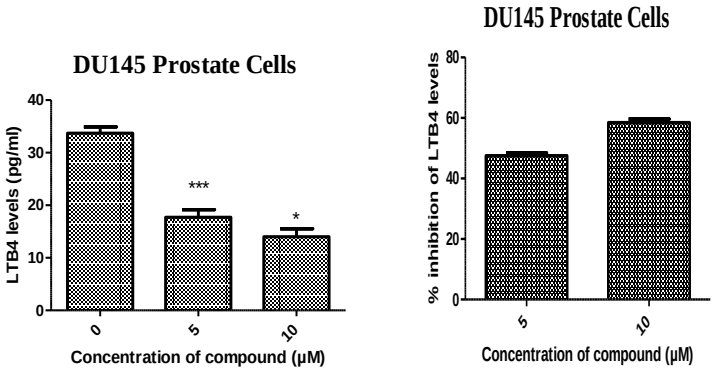

(i) (ii)

Figure 7.22. Effect of dammarane triterpenoid 1on LTB4 levels represented in pg/ml (i) and percent inhibition (ii) in DU145 prostate cancer cells.

7.4.7. Effect of dammarane triterpenoid 1 on PGs levels in DU145 prostate cancer cells

Dammarane triterpenoid 1 inhibited 26.09± 2.80% and 34.87± 2.20% production of PGE_2 levels in DU145 cancer cells at 5µM and 10µM concentrations respectively. **Figure 7.23** represents the inhibitory effect of dammarane triterpenoid 1 on PGE_2 levels in DU145 prostate cancer cells.

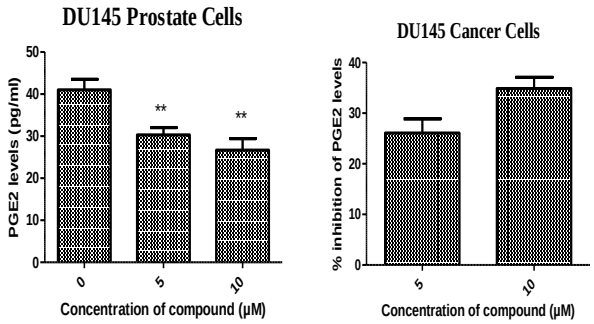

(i) (ii)

Figure 7.23. Effect of dammarane triterpenoid 1on PGE2 levels represented in pg/ml (i) and percent inhibition (ii) in DU145 prostate cancer cells

7.5. DISCUSSION

COX and 5-LOX dual inhibitors have been reported for cytotoxic activities against various cancer cells and these compounds are being developed as cancer chemopreventive and therapeutic agents COX and LOX dual inhibitors block cancer cell proliferation and induce apoptosis in cancer cells. Recently a clinical study suggests that the inhibition of both COX-2 and 5-LOX may be an effective preventive and therapeutic approach for patients with colon cancer (Che et al., 2016). Chebulagic acid from *Terminalia chebula* exhibited anti-proliferative effect on HCT-15, COLO-205 K562, MDA-MB-231, and DU-145 cancer cell lines and induced apoptosis in COLO-205 cancer cells (Reddy et al. 2009). A COX and 5-LOX dual inhibitory Licofelone induced apoptosis in HCA-7 colon cancer cells via intrinsic pathway. However, the role of its effect on AA pathway in apoptosis induction is not clear (Tavolari et al., 2008). A dual COX-2 and 5-LOX inhibitor darbufelone arrested cell cycle of LoVo cancer cells at G0/G1 phase and induced apoptosis in the cells by activating caspases 3 and 9, upregulating Bax as well as downregulating Bcl-2 (Che et al., 2016; Ding et al., 2001; Miroslava et al., 2014; Qi et al., 2012).

In this background, we have carried out anticancer studies of dammarane triterpenoid 1 using MIA PaCa-2 pancreatic, DU 145 prostate, Caco-2 colon, HL-60 leukemia cancer cell line and found good antiproliferative effect against MIA PaCa-2 pancreatic cancer cell line. Dammarane triterpenoid 1 exhibits better antiproliferative effect on cancerous cells than non-cancerous cells. Further pro-apoptotic experiments results, accumulation of sub-G_0 cell population, mitochondria membrane potential loss, elevated cytochrome *c* levels, nuclear morphological changes and DNA fragments formations were found in dammarane triterpenoid 1 (5 µM) treated MIA PaCa-2 pancreatic cancer cells.

Dammarane triterpenoid 1 inhibited cell proliferation of DU145 prostate cancer cells and arrested cell cycle at G0/G1 phase. Mitochondrian membrane potential loss, increase of cytosolic cytochrome *c* and Bax levels, decrease of Bcl-2 levels and enhanced caspases-3 and -9 activities were observed in dammarane triterpenoid 1-treated DU145 prostate cancer cells. Moreover, dammarane triterpenoid 1 caused DNA fragmentation (discrete ladder pattern) in DU145 prostate cancer cells, which is an indication of induction of apoptosis. In intrinsic pathway, anti-apoptotic Bcl-2

family proteins inhibit mitochondrial outer membrane permeabilization (**Figure 7.24**). Pro-apoptotic Bax increases the permeability of mitochondrial outer membrane that leads to mitochondrial membrane potential loss and form mitochondrial apoptosis-induced channels. Followed by cytochrome *c* and other pro-apoptotic proteins are released into cytosol through the mitochondrial membrane pores. The released cytosolic cytochrome *c* activates caspase-9, which in turn activates of caspases cascade including caspase-3 that leads to activation of ultimate biochemical events in apoptosis. These results demonstrated that dammarane triterpenoid 1 induces apoptosis in MIA PaCa-2 pancreatic and DU145 prostate cancer cells via intrinsic pathway (**Figure 7.24**).

COX and 5-LOX catalyze AA into PGs and LTs respectively and promote cell proliferation and inhibit apoptosis in cancer cells (**Figure 7.24**). Previous studies demonstrated that COX and 5-LOX inhibitors exhibit antiproliferative and pro-apoptotic potentials in cancer cells. In present study, dammarane triterpenoid 1 inhibits production of PGs and LTs as well as exhibits antiproliferative and pro-apoptotic potentials in MIA PaCa-2 pancreatic and DU145 prostate cancer cells. Therefore, this study suggests that antiproliferative and pro-apoptotic activities of dammarane triterpenoid 1 due its COX and 5-LOX dual inhibitory potential.

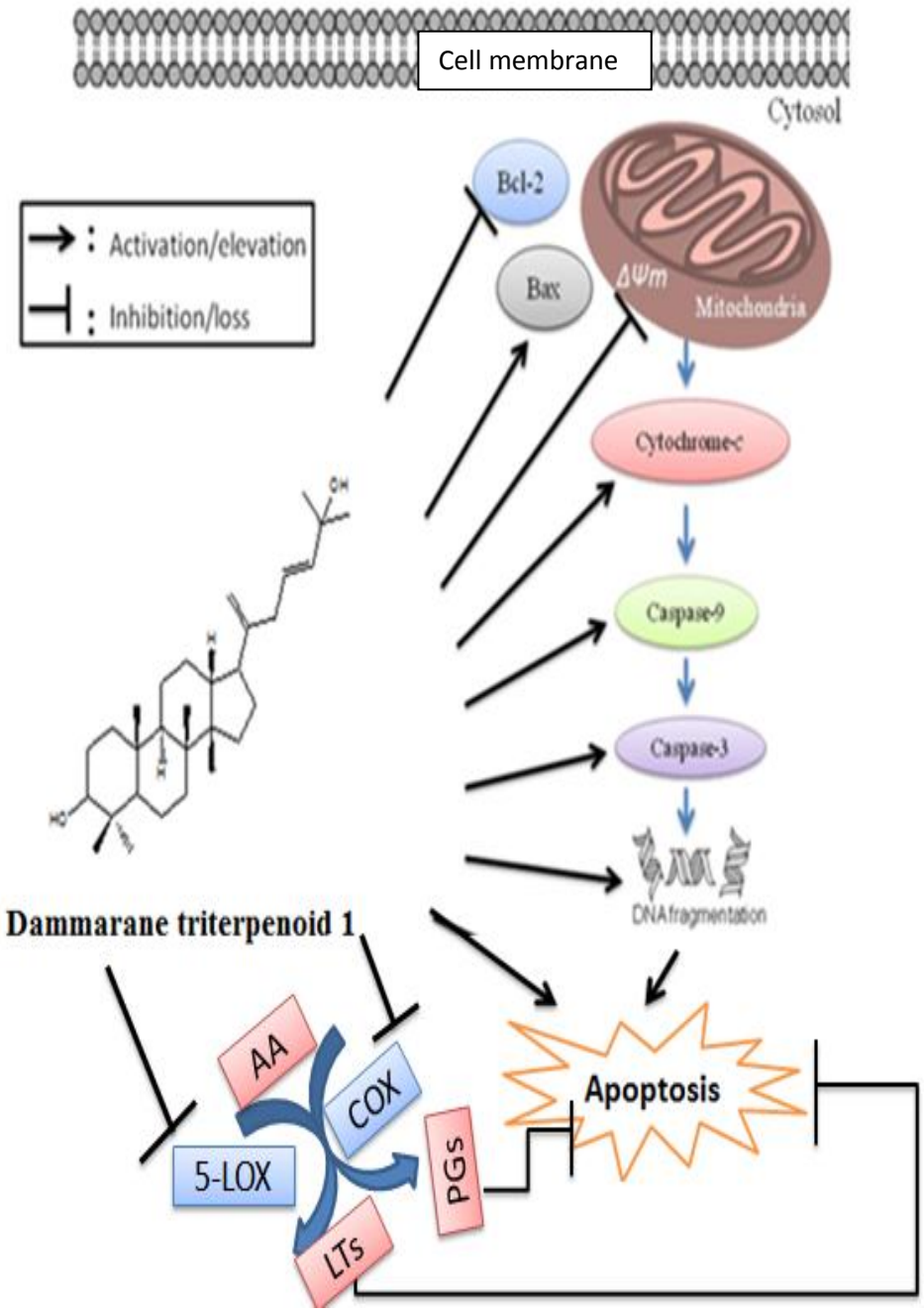

Figure 7.24. Schematic representation of pro-apoptotic effects of dammarane triterpenoid 1 in cancer cells